Phase Identification in a Series of Liquid Crystalline TPP Polyethers and Copolyethers Having Highly Ordered Mesophase Structure. 3. Thin Film Surface-Induced Ordering Structure and Morphology in TPP($n = 7$)

Rong-Ming Ho, Yeocheol Yoon, Mark Leland, and Stephen Z. D. Cheng*

Maurice Morton Institute and Department of Polymer Science, The University of Akron, Akron, Ohio 44325-3909

Dengke Yang

Liquid Crystal Institute, Kent State University, Kent, Ohio 44242-0001

Virgil Percec and Peihwei Chu

Department of Macromolecular Science, Case Western Reserve University, Cleveland, Ohio 44106-2699

Received January 10, 1996; Revised Manuscript Received April 8, 1996[⊗]

ABSTRACT: A series of liquid crystalline polyethers has been synthesized from 1-(4-hydroxy-4′-biphenylyl)-2-(4-hydroxyphenyl)propane and α,ω-dibromoalkanes [TPP(*n*)]. TPP(*n*)s show multiple phase transitions during cooling and heating. In TPP($n = 7$) bulk and fiber samples, three liquid crystalline phases have been identified: nematic phase and highly ordered smectic F and smectic crystal G phases. The detailed structures and morphology of TPP($n = 7$) thin films (with a thickness ranging from 10 to 100 nm) have been studied by electron diffraction and transmission electron microscopy experiments on three different types of substrates. These include silane-grafted, amorphous carbon-coated, and clean glass surfaces. The development of homeotropic molecular alignment in monodomains has been obtained by using substrates with silane-grafted and amorphous carbon-coated surfaces. Both surfaces can also induce structural ordering in TPP($n = 7$) to form an orthorhombic lateral packing which does not exist in the bulk and fiber samples and has only appeared in TPP($n \geq 11$). This phase has been identified as a smectic crystal H phase. It has been found that the monodomain morphology of the highly ordered smectic crystal phases with the homeotropic molecular alignment depends strongly on the structural symmetry. Furthermore, the silane-grafted surface produces better homeotropic molecular alignment for TPP($n = 7$) than the amorphous carbon-coated surface, with the latter demonstrating a continuous change in the chain director between −30° and +30°. This change in the orientation results in observable striations in the monodomain morphology. The origin of this variation in the chain director may be associated with the fact that the vector normal to the layer of the smectic crystal phases is tilted about 32° away from the molecular direction (58° between the molecular direction and the layer surface). The clean glass surface does not induce orthorhombic packing and only polydomain structures can be found in which an in-plane homogeneous alignment of the chain directors exists. On the other hand, mechanically sheared thin films on glass surfaces show a uniaxial homogeneous molecular alignment.

Introduction

For liquid crystalline phases, the molecular direction of preferred orientation is known as the director (vector). A monodomain is described as a region in which the director follows a narrow distribution of orientations. In a monodomain, except for some of the centers of defects, the director cannot exhibit a sudden change leading to a discontinuous first derivative of the director with respect to the spatial coordinate. In polymer liquid crystals the size of a monodomain is more restricted than in small molecule liquid crystals due to the high viscosity and slow molecular motion associated with the long chain nature of polymer molecules. Alignment of the molecules toward one direction is thus difficult to achieve under an external field.

In general, for nematic liquid crystalline polymers the director is typically defined by the mesogenic moieties. In other words, the mesogenic moieties are aligned with respect to the director which is the symmetry axis of the orientation distribution. For a smectic A or C phase, which exhibits a layer structure among the oriented molecular chains, additional structural parameters of the layer structure are necessary to describe the structural order. In highly ordered smectic crystal phases, bond orientational and positional orders are introduced within or even among the layers. In this case, certain degrees of lateral order having a correlation length of over 10 nm are exhibited in addition to the layer structures.[1−3]

Recently, highly ordered smectic crystal phases have been found in a series of main-chain liquid crystalline polyethers synthesized from 1-(4-hydroxy-4′-biphenylyl)-2-(4-hydroxyphenyl)propane and α,ω-dibromoalkanes [TPP(*n*)].[4−6] Phase diagrams of the transition temperatures with respect to the odd and even numbers of methylene units (*n*) have been obtained. The TPP(*n*)s show multiple phase transitions during cooling and heating, and the undercooling dependence of these transitions is found to be small from the differential scanning calorimetry (DSC) measurements. The detailed structural identifications were carried out *via* wide angle X-ray fiber and powder diffraction (WAXD) experiments. The liquid crystalline morphology was also studied utilizing polarized light and transmission electron microscopy (PLM and TEM). All structure

* To whom correspondence should be addressed.
[⊗] Abstract published in *Advance ACS Abstracts,* May 15, 1996.

S0024-9297(96)00031-9 CCC: $12.00

identification was performed on bulk and fiber samples having polydomain structures.[4−6]

In a manner similar to the crystal structure determination in polymer single crystals, it is interesting to explore the structure, order correlation, and morphology based on an investigation of the liquid crystalline polymer monodomains. One way to obtain monodomains in liquid crystalline polymers is to develop a homeotropic orientation of the chain directors perpendicular to the substrate surface. The structure and morphology of liquid crystalline polymers having highly ordered lateral packing can then be studied *via* electron diffraction (ED) and TEM experiments. The alignment is usually carried out in thin films which possess a typical thickness on the order of a few tens of nanometers. One of the aspects which is interesting to us in the study is whether the structural order in these thin film samples is the same as in the bulk samples. It has been reported that in small molecule liquid crystals one may observe surface-induced structural order in the thin films.[7−9] In TPPs, a smectic crystal H (S_H) phase has been identified in bulk and fiber samples of TPP($n \geq 11$)s.[5] This phase possesses an orthorhombic lateral packing perpendicular to the chain direction. Since the layer normal vector is tilted away from the meridian of the fiber patterns, the unit cell appears as monoclinic in the S_H phase with the *c*-axis along the chain director and the *ab*-plane parallel to the layer surface. In the bulk and fiber TPP($n = 7$) samples, on the other hand, the S_G phase, which possesses a hexagonal lateral packing ($a = 0.54$ nm) perpendicular to the chain direction, is stable down to the glass transition temperature. A monoclinic unit cell can also be deduced since a 46° tilting of the layer normal vector and 14° tilting of the chain director with respect to the meridian in WAXD fiber patterns are observed. The S_H phase is not found in TPP($n = 7$).[5] If a surface-induced ordering process occurs in TPP($n = 7$) thin films, the most likely observation in thin films should be an orthorhombic lateral packing perpendicular to the chain direction, similar to that found in TPP($n \geq 11$)s.

Several alignment processes to produce the uniform orientation in small molecule liquid crystals have been reported. The alignment can be induced by processing (*e.g.*, mechanical shearing), chemically or physically modifying surfaces (*e.g.*, grafting chemical groups or rubbing), and/or applying external fields (*e.g.*, electric or magnetic field). Processing-induced orientation, in general, results in a homogeneous orientation in which the mesogenic moieties lie parallel to the substrate surface. In the case of surface-induced orientation, both homogeneous and homeotropic alignments may be obtained *via* a specific surface with chemical or physical modifications.[10] For example, homeotropic alignment can be achieved by grafting silane onto the surface with long alkyl chains.[11,12] Other methods including the use of a surface with strong polarity (*e.g.*, amphiphilic character)[13,14] and a SiO-rotatively evaporated surface[15] may also be exploited to obtain the homeotropic alignment for small molecule liquid crystals. In contrast to small molecules, molecular connectivity between the mesogenic moieties in liquid crystalline polymers may significantly affect this orientation process. Nevertheless, a homeotropic orientation of a thermotropic liquid crystalline copolyester has also been achieved on rock salt substrate by Donald *et al.*[16−18] On the basis of TEM results, they concluded that the chemical nature of the substrate has a pronounced effect on the morphology.

In this paper, we report our attempt to study the structure and morphology of a liquid crystalline polyether having highly ordered smectic crystal phases using TEM and ED experiments. In order to identify the lateral packing symmetry of the highly ordered smectic crystal phases in TPP($n = 7$) thin films and substrate surface effects on these phase structures, different surfaces including silane-grafted, amorphous carbon-coated, and clean glass surfaces are utilized to induce specific chain alignment of the liquid crystalline TPP($n = 7$). The chemical structure of this polyether TPP($n = 7$) is

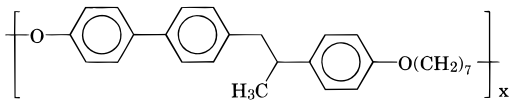

Experimental Section

Materials and Samples. TPP($n = 7$) was synthesized from 1-(4-hydroxy-4′-biphenylyl)-2-(4-hydroxyphenyl)propane and α,ω-dibromoheptane. The detailed synthetic procedure has been reported in an earlier publication.[19] The number average molecular weight is 25 000 g/mol, and the polydispersity is 2.6 measured by gel permeation chromatography (GPC) in chloroform based on polystyrene standards.

Various procedures were used to prepare the TPP($n = 7$) thin films (10−100 nm) for TEM and ED experiments. On the amorphous carbon-coated surfaces, TPP($n = 7$) thin films were cast from a 0.1% (w/w) TPP($n = 7$)/chloroform solution. After the solvent evaporated under vacuum, the samples were heated to the temperature of the nematic state for 15 h under a dry nitrogen atmosphere. Samples were then either slowly cooled or quenched in liquid nitrogen to yield solid thin film samples. The films were then stripped, floated onto the surface of water, and recovered with copper grids.

For clean glass surfaces, the same solution was directly deposited onto the glass slides. The solvent was then evaporated under vacuum. The same thermal history was applied to the samples as described above. For mechanical shearing, TPP($n = 7$) thin films were placed between two glass slides and mechanically sheared at the temperature of the nematic state. After shearing, the samples were quenched in liquid nitrogen. They were stripped using poly(acrylic acid) (PAA), floated onto the surface of water, permitting the PAA to dissolve, and again recovered using copper grids.

In the case of silane-grafted surfaces, TPP($n = 7$) thin films were prepared by casting 0.1% (w/w) TPP($n = 7$)/chloroform solution directly onto the surface of water. After the evaporation of solvent, the TPP($n = 7$) thin films were recovered on silane-grafted glass slides. Again, the same thermal history and the sample recovery procedure were used. To prepare the silane-grafted surfaces on glass substrates, (3-aminopropyl)-triethoxysilane was first dissolved in toluene to obtain a 0.25% (w/w) concentration. The solution was spin-coated onto the glass substrate at 4000 rpm for 20 s. The substrate was then heated at 100 °C for 2 h to evaporate the solvent and to carry out the reaction of silane with SiO on the glass surface. In order to examine the effect of the water surface casting, the same procedure for TEM sample preparation was also conducted for thin films on the amorphous carbon-coated and clean glass substrate surfaces.

For wide angle X-ray diffraction (WAXD) measurements, TPP($n = 7$) thin and thick films having thicknesses of about 300 nm and 1 mm, respectively, were prepared by casting the TPP($n = 7$)/chloroform solution at 80 °C. The solvent was then evaporated in a vacuum oven. The same thermal history described above was applied to the film samples.

Instrumentation and Experiments. The structures and morphology of TPP($n = 7$) thin films on different substrates

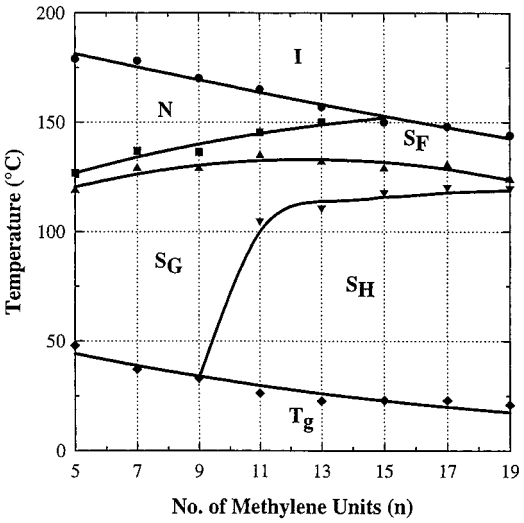

Figure 1. Phase diagram of TPP(n = odd)s.

were observed using a JEOL (JEM 1200 EX II) TEM with an accelerating voltage of 120 kV. The TPP($n = 7$) thin films were shadowed with Pt and coated with carbon for TEM morphological observations. A tilting stage was used for the ED experiments to determine the molecular alignment on the different types of substrates. Calibration of the ED spacings was carried out using gold (Au) and thallium chloride (TlCl) (d spacing < 0.384 nm, the largest spacing for TlCl). Spacing values larger than 0.384 nm were calibrated by doubling the d spacings of those reflections based on the spacing of their first-order reflections. Correlation lengths of each *(hk0)* plane were also determined for ED patterns from the Scherrer equation as a first approximation.

Reflection WAXD experiments were conducted with a Rigaku 12 kW rotating-anode generator (Cu Kα) with a diffractometer. The X-ray beam was monochromatized using a graphite crystal. The 2θ angle region ranged between 2° and 35° with a scanning rate of 0.1°/min. The diffraction peak positions and widths observed from WAXD experiments were calibrated through silicon crystals with known crystal sizes.

Results and Discussion

Surface-Induced Ordering Process. From our previous work, it was found that TPP(n = odd)s show complicated phase behavior. A complete phase diagram was obtained and reported in ref 5. Figure 1 is a reproduced phase diagram for the purpose of understanding the phase behavior in TPP(n = odd)s. It is evident that highly ordered smectic phases exist for TPP($n = 7$) and the transition sequence from high temperature to room temperature is[5]

$$\mathrm{I} \xrightarrow[6.21\ \mathrm{kJ/mol}]{178\ ^\circ\mathrm{C}} \mathrm{N} \xrightarrow[3.45\ \mathrm{kJ/mol}]{137\ ^\circ\mathrm{C}} \mathrm{S_F} \xrightarrow[2.78\ \mathrm{kJ/mol}]{129\ ^\circ\mathrm{C}} \mathrm{S_G}$$

The transition temperatures as well as heats of transitions are also given for complete information. Note that these results were obtained in TPP($n = 7$) bulk (three-dimensionally isotropic thick films having a thickness of 1 mm) and fiber (one-dimensionally oriented samples with a diameter of 10 μm) samples.[5] Therefore, they represent the bulk phase behavior without any surface effects.

The first question is whether the highly ordered smectic structures (S_F and S_G which show virtually the same lattices with different order correlation lengths[5]) can also be observed in TPP($n = 7$) thin films. When TPP($n = 7$) thin film samples on the amorphous carbon-coated substrate are slowly cooled (0.1 °C/min) from the nematic phase to room temperature, sharp, single crystal-like ED diffraction can be obtained from a monodomain structure, as shown in Figures 2 and 3. These results indicate the existence of highly ordered lateral packing and homeotropic chain arrangement in TPP($n = 7$) thin films. This indicates that the ED patterns possess a [00l] zone. According to the *(hk0)* reflections of ED patterns in Figure 2, the lateral packing symmetry is hexagonal with dimensions of $a = b = 0.51$ nm, suggesting that a S_G phase exists (which possesses a hexagonal lateral packing perpendicular to the chain direction). This result is consistent with the WAXD experimental observations in TPP($n = 7$) bulk and fiber samples, as shown in Figure 4a and in ref 5, and a monoclinic unit cell can be deduced when the *ab*-plane is parallel to the layer surface.[5]

In addition to the hexagonal lateral packing, an orthorhombic lateral packing can also be identified from our ED observations, as shown in Figure 3. This lateral packing has a lattice size of $a = 0.80$ nm and $b = 0.53$

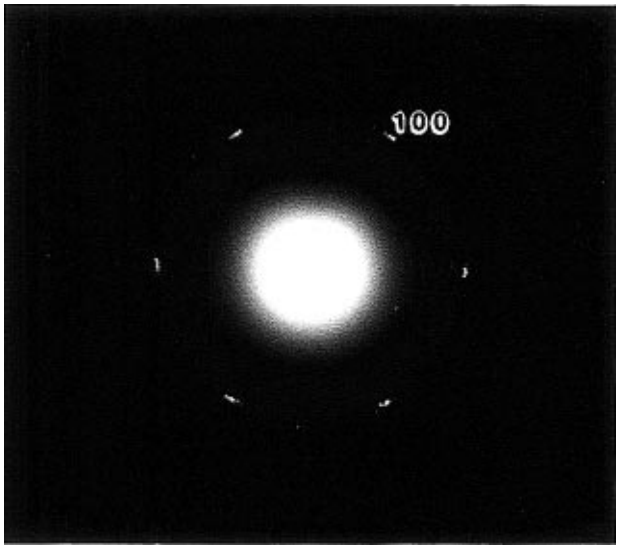

Figure 2. ED patterns for TPP($n = 7$) thin film samples on amorphous carbon-coated substrate surfaces with hexagonal lateral packing obtained from the monodomain along the [00l] zone.

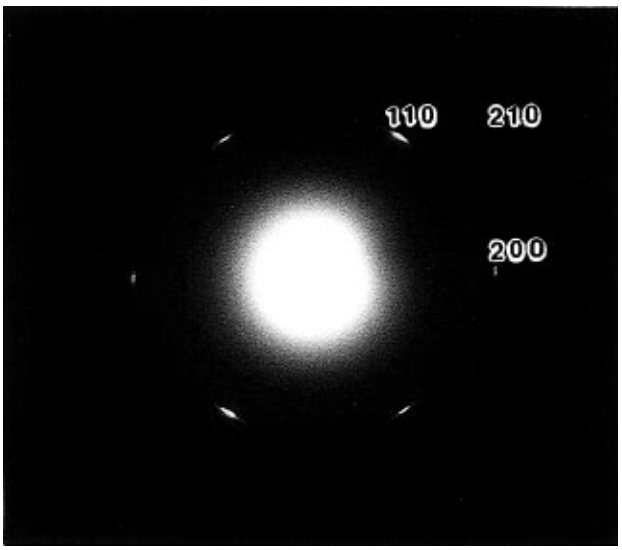

Figure 3. ED patterns for TPP($n = 7$) thin film samples on amorphous carbon-coated substrate surfaces with orthorhombic lateral packing obtained from the monodomain along the [00l] zone.

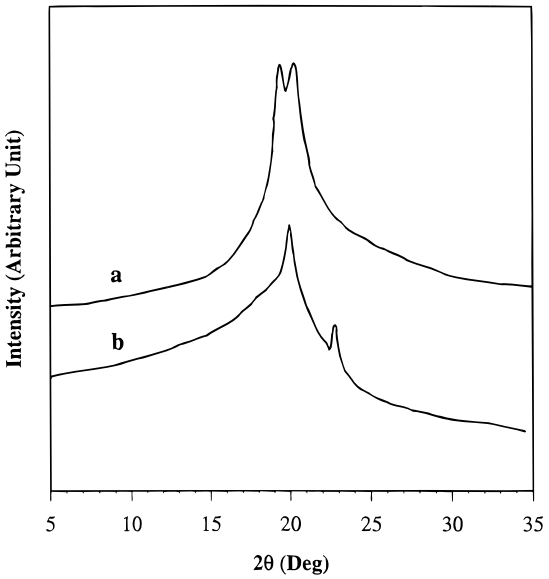

Figure 4. WAXD powder pattern for TPP(n = 7) (a) bulk samples having a thickness of about 1 mm and (b) thin film samples having a thickness in a 300 nm range.

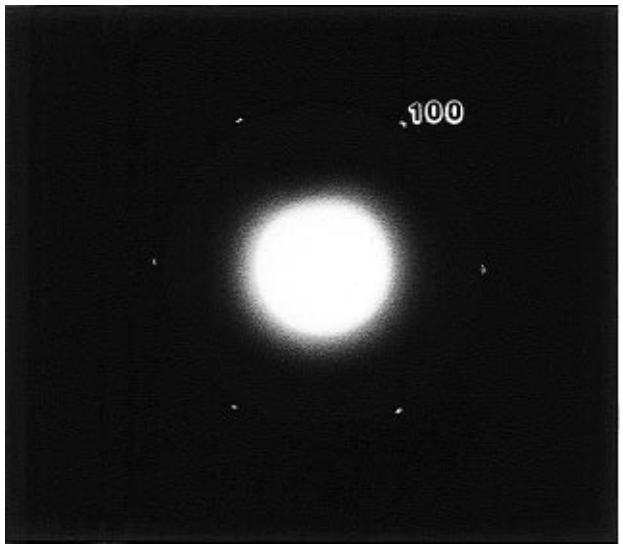

Figure 5. ED patterns for TPP(n = 7) thin film samples on silane-grafted surfaces with hexagonal lateral packing obtained from the monodomain along the [00l] zone.

nm based on the (200) and (110) reflections, and it has not been observed in TPP(n = 7) bulk and fiber samples. Since thin films having a thickness of 10−100 nm possess a large amount of surface area, one predicts that this surface may substantially affect the structural ordering *via* the "surface-induced ordering process". The presence of this orthorhombic packing seems to be unique to the thin film samples. Interestingly, the b-dimension of the lateral packing in Figure 3 is the same as for the orthorhombic lateral packing found in the S_H phase of TPP($n \geq 11$)s, while the a-dimension is also close to those of other TPP(n = odd)s ($a^* \sin \beta$, where a^* is the a-axis of the monoclinic unit cell and β is the angle between the a^*- and c-axes in the unit cell and here is 130°).[5] A corresponding WAXD pattern for TPP(n = 7) thin films can also be obtained, as shown in Figure 4b. A significant reflection at 2θ = 22.8° is identified to be a (200) reflection for the orthorhombic lateral packing and is consistent with the ED pattern. Obviously, the structural order in these thin film samples is different from that in the bulk samples. The

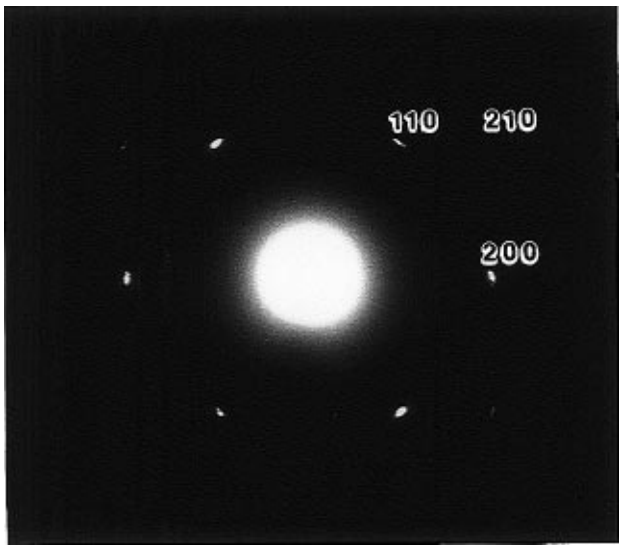

Figure 6. ED patterns for TPP(n = 7) thin film samples on silane-grafted surfaces with orthorhombic lateral packing obtained from the monodomain along the [00l] zone.

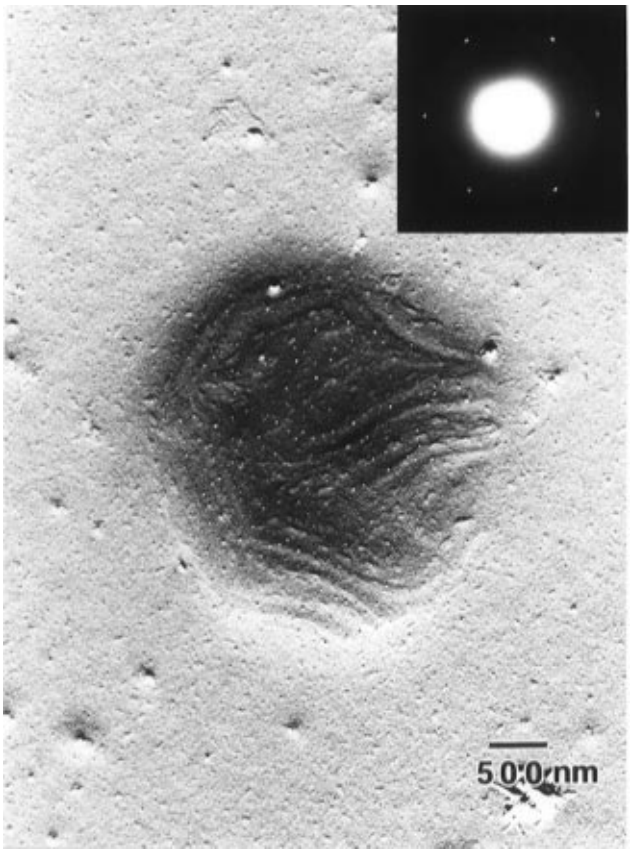

Figure 7. TEM observations of the TPP(n = 7) monodomain of the hexagonal lateral packing grown on the amorphous carbon-coated surfaces. The ED pattern originates from the monodomain and is shown with the correct orientation.

polymer−substrate interaction caused by the surface energies in the thin film samples should be an important factor for the surface-induced structural ordering in TPPs. This phenomenon must be similar to the behavior in small molecule liquid crystals.

In addition, the ED patterns provide an opportunity to quantitatively estimate the lateral correlation lengths of the different reflection planes using the Scherrer equation as a first approximation. For the hexagonal packing the correlation length of the (100) planes is 10

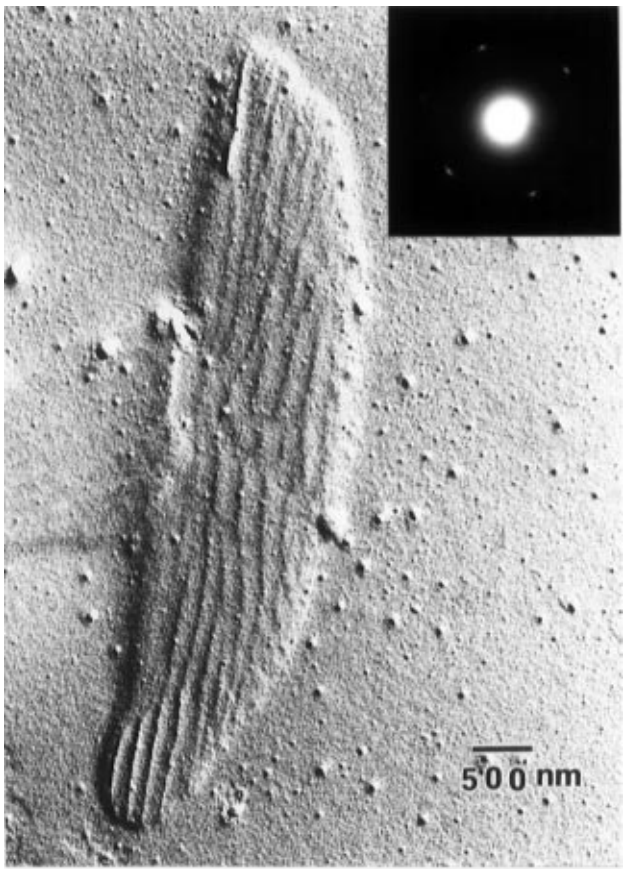

Figure 8. TEM observations of the TPP($n = 7$) monodomain for the orthorhombic lateral packing grown on the amorphous carbon-coated surfaces. The ED pattern originates from the monodomain and is shown with the correct orientation.

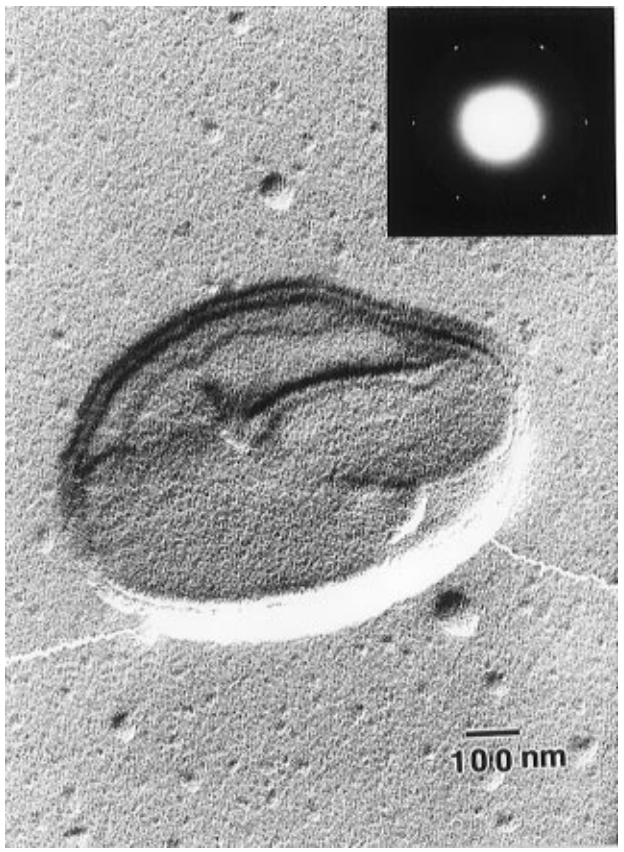

Figure 9. TEM observations of the TPP($n = 7$) monodomain for the hexagonal lateral packing grown on the silane-grafted surfaces. The ED pattern originates from the monodomain and is shown with the correct orientation.

nm, which corresponds well to the result obtained from WAXD experiments in the S_G phase of TPP($n = 7$).[5] On the other hand, the correlation lengths of the (200) and (110) planes in the orthorhombic packing are 10 and 12 nm, respectively. These values are comparable to those found in the S_H phase of TPP($n \geq 11$)s.[5]

Similar observations are found for TPP($n = 7$) thin films on the silane-grafted surface. After the same thermal treatment, two *(hk*0*)* ED patterns representing a hexagonal and orthorhombic lateral packing can also be obtained (Figures 5 and 6). However, in the thin films on a clean glass surface, only a diffuse ring pattern is found, indicating a polydomain structure. The *d* spacing of the ring is in the vicinity of 0.45 nm, which corresponds to the (110) and (200) reflections in the S_G hexagonal packing (see below in Figure 11). No reflections generated from an orthorhombic packing can be seen, indicating that on the glass surface, the surface-induced ordering process is at least not as predominant as those on the silane-grafted and amorphous carbon-coated surfaces.

Surface Effects on Chain Alignment. Silane-grafted, amorphous carbon-coated, and clean glass substrates have been used to examine the surface effects on the TPP($n = 7$) chain alignment. On the amorphous carbon-coated surface, both the hexagonal and the orthorhombic ED patterns along the [00*l*] zone appearing in Figures 7 and 8 can be obtained under the continuously tilted angles ranging from 30° counterclockwise to 30° clockwise with respect to the substrate surface normal. This seems to indicate that the chain director in the liquid crystalline phase may deviate from the homeotropic alignment by ±30° such that the deviation is continuous. Moreover, striations on the surfaces of both monodomains can be seen. In particular, the striations in Figure 8 are oriented along the long axis (*b*-axis in the orthorhombic packing, see below) of the domain. We speculate that the striations in the morphological observations in Figures 7 and 8 may be attributed to this type of deviation from the perfect homeotropic orientation. The reason for the tilting of the chain directors is not yet fully understood. This must be caused by the formation of liquid crystalline defects. Note that in TPP($n = 7$) the layer normal vector is tilted 46° and the chain director is tilted 14° away from the meridian of the fiber pattern.[5] If the layer surface is parallel to the substrate surface, the chain direction should have a 32° tilt away from the substrate surface normal. This may provide the limits of the tilting angles of the chain director away from the homeotropic arrangement. As a result, this observation may be associated with the packing arrangement of the smectic layers on the substrate surface.

In contrast to the carbon-coated surfaces, the silane-grafted substrate surfaces possess alkyl chains which exhibit a uniform homeotropic orientation. This uniform orientation of TPP($n = 7$) for both the hexagonal and the orthorhombic lateral packings is identified by ED patterns along the [00*l*] zone, as shown in Figures 9 and 10. No *(hk*0*)* ED patterns are obtained through any tilting angles. Furthermore, no striations can be observed in the monodomain morphology. This indicates that the homeotropic arrangement of the chain directors is nearly perfect for the silane-grafted surfaces, and it is consistent with the interpretation of the striation formation observed for monodomains on the amorphous carbon-coated surfaces.

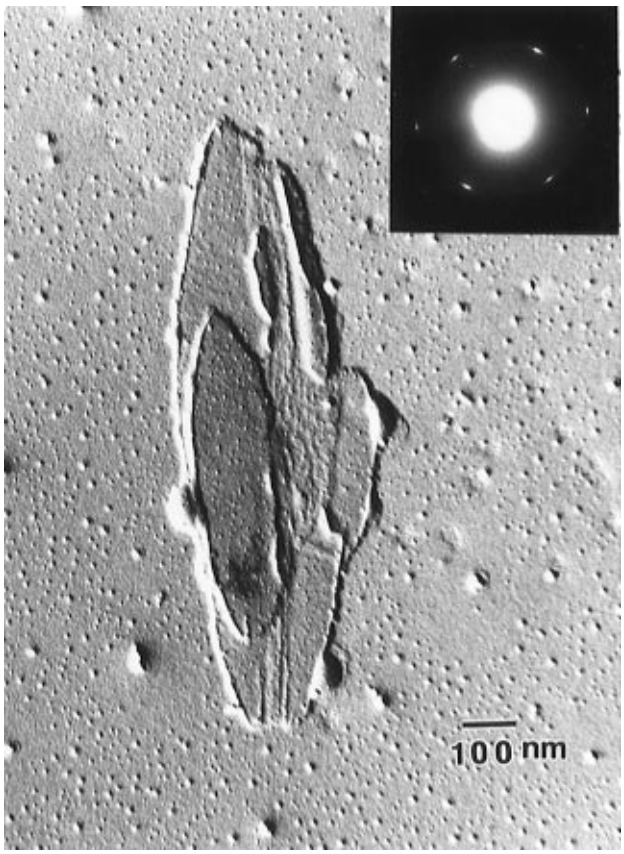

Figure 10. TEM observations of the TPP($n = 7$) monodomain for the orthorhombic lateral packing grown on the silane-grafted surfaces. The ED pattern originates from the monodomain and is shown with the correct orientation.

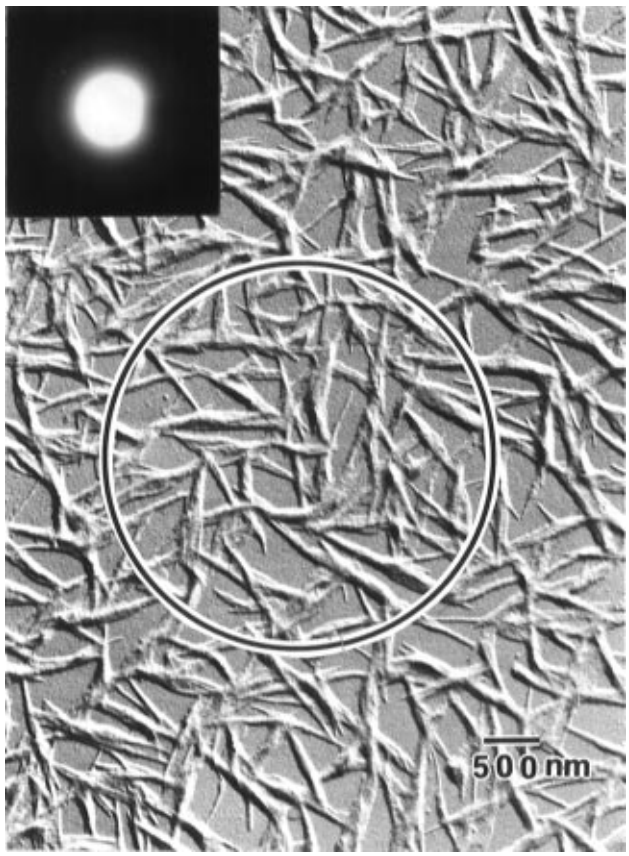

Figure 11. TEM micrograph of a TPP($n = 7$) thin film sample on a glass surface without mechanical shearing. The ED pattern originates from the circled area of the micrograph.

On the clean glass surface, the morphology of TPP($n = 7$) thin films without mechanical shearing is shown in Figure 11. The samples have undergone the same thermal treatment; namely, they were slowly cooled (0.1 °C/min) to room temperature from the nematic phase. A randomly distributed network type of morphology can be found, and thus, only a ring pattern is obtained from ED having a d spacing in the vicinity of 0.45 nm (included in Figure 11). As described previously, this is attributed to the hexagonal lateral packing with the (110) and (200) reflections. We suggest that the development of this morphology is attributed to a high nucleation density induced by the glass surfaces and a more or less homogeneous molecular arrangement is formed. The molecular chains are mainly parallel to the glass surface, while the chain directors are randomly oriented within the thin films. This phenomenon may thus represent an "in-plane" homogeneous arrangement. The effect of the surface-induced ordering process is not significant, and only hexagonal lateral packing can be found.

On the other hand, for TPP($n = 7$) thin films on a glass surface with mechanical shearing, Figure 12 shows the lamellar normal direction is $\pm 46(\pm 2°)$ with respect to the shear direction, which represents the layer structure of the smectic crystal phase and is responsible for the four smectic layer quadrant reflections in the low-angle region observed in the WAXD fiber patterns.[5] The molecular chain direction is about $\pm 14°$ with respect to the shear direction. Furthermore, the ED pattern included in Figure 12 possesses the same high-angle reflections as observed in the WAXD fiber pattern.[5] This indicates that a uniaxial homogeneous arrangement has been achieved during the mechanical shearing. The layers perpendicular to the shear direction possess a spacing of 0.5−1 μm and correspond to the banded texture observed under PLM.[5]

One may argue that the homeotropic orientation found on the silane-grafted surfaces may be attributed to the effect of the water surface casting. In order to examine this possibility, TPP($n = 7$) thin films were prepared on clean glass and carbon-coated surfaces using the same water surface casting procedure. No significant differences in the molecular orientation, lateral packing, and morphology are apparent. Therefore, water surface casting does not appear to have a major impact on the observed morphology and structures of the thin film samples. We expect that the main cause of the different orientational arrangements must be from the surface energies of TPP($n = 7$) and substrate surfaces as well as their interactions.

Lateral Packing Symmetry and Morphology. The morphology corresponding to the hexagonal and orthorhombic lateral packing on the amorphous carbon-coated surface is shown in Figures 7 and 8, respectively. Since molecular alignment in the monodomain is more or less homeotropic, the monodomain shape should be representative of macroscopic habits of the lateral packing. It is interesting to observe that a circular morphology can be found for the hexagonal packing (Figure 7), while an elongated morphology is observed for the orthorhombic packing (Figure 8). Based on the corresponding ED patterns, the elongated direction coincides with the b-axis of the orthorhombic packing. These results suggest that the preferential lateral growth direction for the orthorhombic packing is along the b-axis while an isotropic lateral growth can be found for the hexagonal packing.

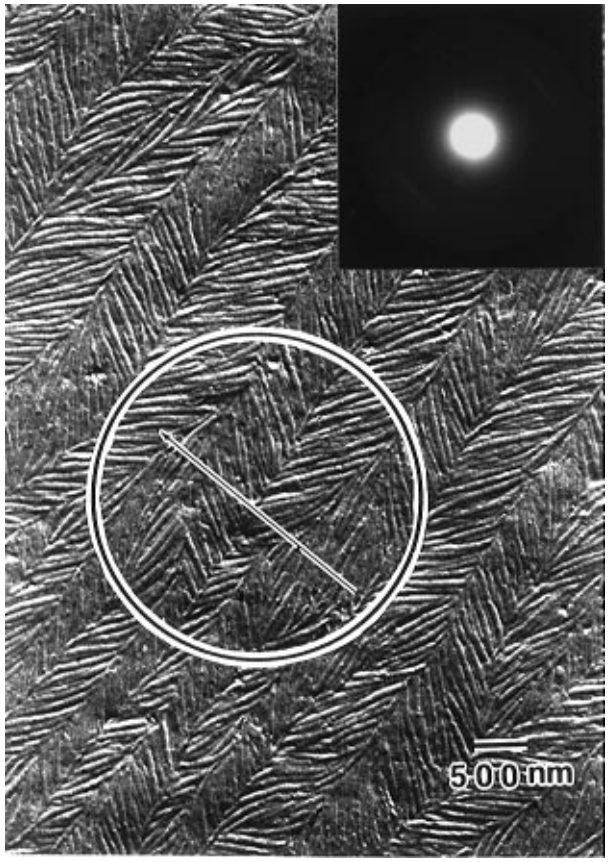

Figure 12. TEM micrograph of the TPP($n = 7$) thin film sample on a glass surface with mechanical shearing. The ED pattern originates from the circled area of the micrograph and is shown with the correct orientation.

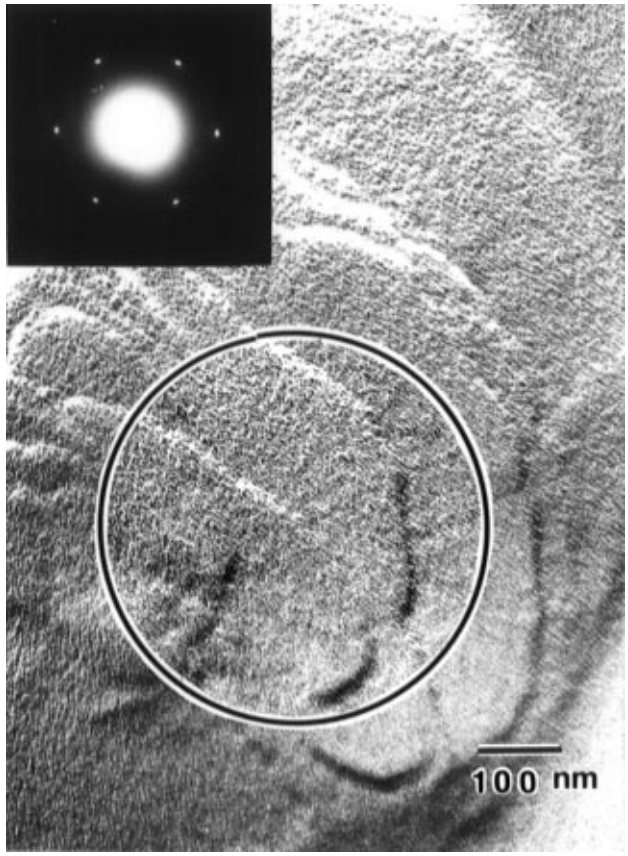

Figure 13. TEM observations of the TPP($n = 7$) multiple layer morphology with the hexagonal lateral packing grown on the silane-grafted surfaces. The ED pattern originates from the circled area of the monodomain and is shown with the correct orientation.

TPP($n = 7$) thin films on the silane-grafted surfaces also show a similar correspondence of the monodomain morphology with the two types of lateral packing. On the basis of the *(hk*0*)* ED patterns included in these figures, the homeotropic arrangement of the chain directors can be clearly identified (having the [00*l*] zone in these ED patterns). In the case of hexagonal packing, the monodomain shows a circular shape, while in the orthorhombic packing an elongated shape is observed with the long axis parallel to the *b*-axis. It is evident that the appearance of native monodomain habits in the form of homeotropic TPP($n = 7$) is strongly dependent on the structural symmetry. We note that the habits are similar to the morphological observations in the lamellar single crystals. In general, regularly polygonal lamellae occur only in polymers in which the unit cells exhibit 3-, 4-, or 6-fold rotational symmetry about the chain axes. Crystals of lower symmetry often adopt ribbon-like habits because of much faster growth along one unique axis.[20] The single lamellar crystal morphology is, thus, controlled by the structural symmetry. For crystallization, however, the variation in the morphology is also dependent upon the crystallization mechanism, conditions (*e.g.* temperature), and molecular mobility (namely, molecular weight).[21] Compared to the crystallization process, the small undercooling dependence of liquid crystal formation suggests that the structural symmetry plays a more dominant role in the monodomain morphology.

In order to identify the phase behavior of the highly ordered lateral packing, TPP($n = 7$) thin films on the amorphous carbon-coated surfaces were also quenched in liquid nitrogen rather than slowly cooled from the nematic state. The quenched samples exhibit structure and morphology very similar to those of the slowly cooled samples. This indicates that the formation of the highly ordered lateral packing is almost cooling-rate independent, which is one of the general characteristics of the liquid crystalline behavior. These results are consistent with the previous DSC experiments reported in which the undercooling dependence of these transitions in TPPs was found to be small.[4−6] Therefore, the existence of a highly ordered smectic crystal phase is also confirmed by the morphological observations in these structural identification experiments. Similar results were also obtained for the TPP($n = 7$) thin films on silane-grafted surfaces.

It is important to note that the thin films were cooled from the liquid-like nematic phase. When the polymers enter the highly ordered smectic phases, they exhibit a solid-like behavior, indicating a drastic reduction of molecular motion and an increase in the structural ordering. As a result, one may speculate that the morphology observed in Figures 7−10 should be formed directly from the nematic phase. In other words, the orthorhombic lateral packing should be directly formed from the nematic phase due to the surface-induced ordering process rather than from the S_G phase, as indicated in the phase diagram (Figure 1) for the TPP-($n \geq 11$) bulk and fiber samples. Further experiments are necessary to investigate the detailed molecular mechanism and thermodynamic properties of this surface-induced ordering process.

Another interesting observation in the thin-film samples is the stacked lamellar morphology of monodomains for both the hexagonal and orthorhombic

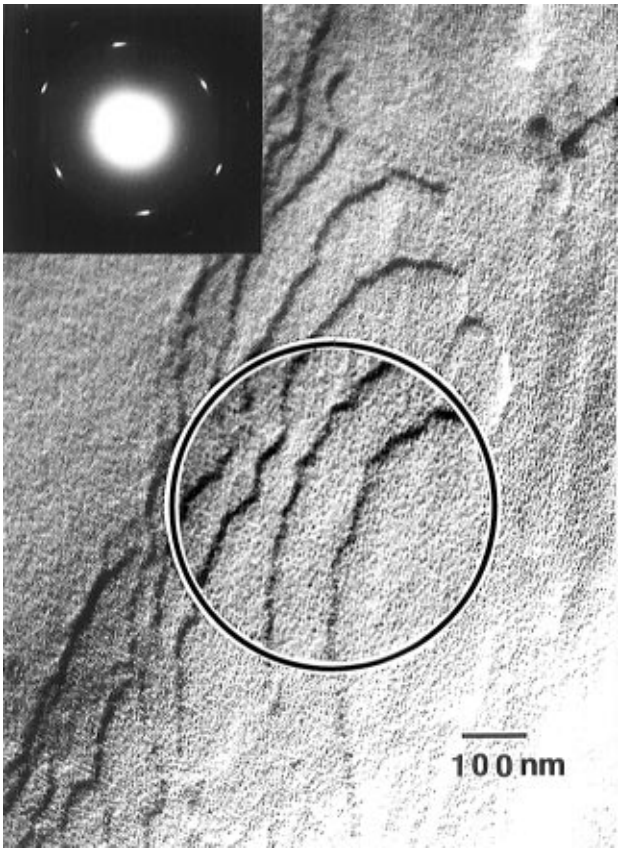

Figure 14. TEM observations of the TPP($n = 7$) multiple layer morphology with the orthorhombic lateral packing grown on the silane-grafted surfaces. The ED pattern originates from the circled area of the monodomain and is shown with the correct orientation.

structures, as shown in Figures 13 and 14. In these cases, the molecular chains exhibit the homeotropic alignment, as identified in the included *(hk*0*)* ED patterns. A rough estimate of the lamellar thickness is 10 nm based on the TEM observations. According to the molecular weight of TPP($n = 7$), the extended chain length should be about 150 nm. The lamellar thickness is thus smaller than the extended chain length. This observation results in an argument about the chain conformation in the highly ordered smectic crystal phases. We suggest that at least some chain folding occurs in the formation of these phases. Further experimental evidence is needed in order to study the detailed chain folding behavior.

Conclusions

Surface effects on the formation of highly ordered smectic crystal phases in TPP($n = 7$) have been investigated *via* three different types of substrates: silane-grafted, amorphous carbon-coated, and clean glass surfaces. It has been found that both silane-grafted and amorphous carbon-coated surfaces induce structural ordering by introducing an orthorhombic lateral packing in TPP($n = 7$) which has not been observed in the bulk and fiber samples. However, this phase has been found in samples with an odd number of methylene units equal to or larger than 11. Both surfaces generate homeotropic chain alignment and form monodomain structures having a size on the order of micrometers. The lateral packing symmetries of these two structures are found to correspond to the monodomain habits. However, the homeotropic alignment induced by the silane-grafted surfaces is more perfect than that by the amorphous carbon-coated surfaces since the latter shows a continuous deviation of the chain directors between $-30°$ and $+30°$ with respect to the substrate surface normal. This may be attributed to the smectic layer structure arrangement on the surface. On the other hand, the clean glass surface only produces polydomain structures and the chain directors mainly exhibit an in-plane homogeneous alignment. Only after mechanical shearing do the molecules on this surface possess a uniaxial homogeneous arrangement. The reason for these different orientational arrangements may depend on surface energies of the polymer and substrate surfaces as well as their interactions.

Acknowledgment. This research was supported by S.Z.D.C.'s Presidential Young Investigator Award from the National Science Foundation (DMR 91-57738).

References and Notes

(1) Gray, D. G. In *Polymeric Liquid Crystals*; Blumstein, A., Ed.; Plenum: New York, 1985.
(2) Pershan, P. S. *Structure of Liquid Crystal Phases*; World Scientific Publishing: Singapore, 1988.
(3) Donald, A. M.; Windle, A. H. *Liquid Crystalline Polymers*; Cambridge: New York, 1992.
(4) Cheng, S. Z. D.; Yoon, Y.; Zhang, A.-Q.; Savitski, E. P.; Park, J.-Y.; Percec, V.; Chu, P. *Macromol. Rapid Commun.* **1995**, *16*, 533.
(5) Yoon, Y.; Zhang, A.; Ho, R.-M.; Cheng, S. Z. D.; Percec, V.; Chu, P. *Macromolecules* **1996**, *29*, 294.
(6) Yoon, Y.; Ho, R.-M.; Li, F.-M.; Cheng, S. Z. D.; Percec, V.; Chu, P. *Macromolecules* **1996**, *29*, xxxx.
(7) Sirota, E. B.; Pershan, P. S.; Sorensen, L. B.; Collett, J. *Phys. Rev. A* **1987**, *36*, 2890.
(8) Tweet, D. J.; Holyst, R.; Swanson, B. D.; Stragier, H.; Sorensen, L. B. *Phys. Rev. Lett.* **1990**, *65*, 2157.
(9) Galerne, Y.; Liebert, L. *Phys. Rev. Lett.* **1991**, *66*, 2891.
(10) Uchida, T. *Mol. Cryst. Liq. Cryst.* **1985**, *123*, 15.
(11) Haller, I. *Appl. Phys. Lett.* **1974**, *24*, 349.
(12) Uchida, T.; Ishikawa, K.; Wada, M. *Mol. Cryst. Liq. Cryst.* **1980**, *60*, 37.
(13) Ohgawara, M.; Uchida, T.; Wada, M. *Mol. Cryst. Liq. Cryst.* **1981**, *74*, 227.
(14) Uchida, T.; Ohgawara, M.; Shibata, Y. *Mol. Cryst. Liq. Cryst.* **1983**, *98*, 146.
(15) Hiroshima, K. *Jpn. J. Appl. Phys.* **1982**, *21*, L791.
(16) Donald, A. M. *Polym. Commun.* **1986**, *27*, 18.
(17) Donald, A. M.; Windle, A. H. *J. Mater. Sci.* **1984**, *19*, 2085.
(18) Donald, A. M.; Windle, A. H. *Polymer* **1984**, *25*, 1235.
(19) Percec, V.; Chu. P.; Ungar, G.; Cheng, S. Z. D.; Yoon, Y. *J. Mater. Chem.* **1994**, *4*, 719.
(20) Keith, H. D.; Padden, F. J., Jr. *Polymer* **1986**, *27*, 1463.
(21) Keith, H. D.; Padden, F. J., Jr. *J. Appl. Phys.* **1964**, *35*, 1270.

MA9600318